Food Research International 203 (2025) 115797

Contents lists available at ScienceDirect

Food Research International

journal homepage: www.elsevier.com/locate/foodres

Oil mobility in sucrose-in-oil dispersions as a function of particle morphology and BET surface

Hilke Schacht [a,*], Lena Trapp [b], Maike Föste [a], Isabell Rothkopf [a], Gisela Guthausen [b,c]

[a] Fraunhofer Institute for Process Engineering and Packaging IVV, 85354 Freising, Germany
[b] Institute of Mechanical Process Engineering and Mechanics, Karlsruhe Institute of Technology, 76131 Karlsruhe, Germany
[c] Engler-Bunte-Institut, Water Chemistry and Technology, Karlsruhe Institute of Technology, 76131 Karlsruhe, Germany

ARTICLE INFO

Keywords:
Oil mobility
Oil immobilization
Dispersion
Sucrose
Edible oils
BET surface
Oil diffusion

ABSTRACT

Solid particles in dispersions, for example sucrose, can reduce the mobility of liquid oils, potentially through sorption or physical entrapment. So far, little is known about the mechanisms and influencing factors behind oil immobilization. Fatty acid composition of oils and the sucrose characteristics (particle size, morphology, BET surface) are thought to affect oil immobilization in sucrose-in-oil dispersions.

For this purpose, dispersions were prepared using four refined oils (coconut, peanut, rapeseed and sunflower oil) and four sucroses (powdered sucrose, granular fine and coarse sucrose and cotton candy). The oils varied in their fatty acid composition, viscosity, and diffusion coefficient, while the sucrose samples differed in their BET surface, particle size, and morphology. To investigate the influence of these properties on oil immobilization, the sucrose-in-oil dispersions were examined across different length scales using oil binding capacity, flow behavior, viscosity and wettability (macroscopic scale), as well as oil diffusion (molecular scale).

Oil immobilization in sucrose-in-oil dispersions was affected stronger by the sucrose properties, especially their morphology and BET surface, than by the oil properties. On a macroscopic level, cotton candy showed the highest oil immobilization, followed by powdered sucrose. On a molecular level, oil diffusion was hindered most by powdered sucrose, while the geometric hindrance was smallest in dispersions with cotton candy.

1. Introduction

Confectionary fat-continuous food products, such as spreads, consist – crudely speaking – of a dispersion of particles, e.g. sucrose, crushed nuts, milk powder and cocoa powder, in a continuous oil phase (Shakerardekani et al., 2013). The processability and shelf life of these products depend on the mobility of the continuous oil phase, which in turn relies on the interactions between the oil and the dispersed particle phase. The flow properties that are important for processability, such as pumping and dosing, depend on the availability of mobile oil, often referred to as “free oil”. On the other hand, mobile oil potentially leads to quality losses in fatty foods, for example de-oiling of spreads, or fat bloom on chocolates with oil-containing fillings (Ereifej et al., 2005; Büschelberger et al., 2015; Rothkopf and Danzl, 2015). Possible ways of oil immobilization are assumed to be physical entrapment (Vignolles et al., 2007; Trapp et al., 2023), adsorption (Abdelwahab et al., 2017; Ifelebuegu and Johnson, 2017) and absorption (Lumanlan et al., 2020; Purwitasari et al., 2023).

Previous research has focused primarily on the immobilization of semi-solid or solid fats, such as cocoa butter or palm fat (Hubbes et al., 2020a, 2020b), as well as on the influence of emulsifiers on these interactions (Johansson and Bergenståhl, 1992a, 1992b; Babin et al., 2005; Argudo et al., 2022). However, little is known so far about the immobilization of unsaturated liquid oils by sucrose particles with varying physicochemical properties, especially in the absence of other substances. Understanding these mechanisms and how the properties of oils and sucrose influence them is essential due to the growing interest in replacing saturated fats with unsaturated oils, where the lack of structure remains a significant challenge (Büschelberger et al., 2015; Martínez et al., 2023; Das and Das, 2024). Additionally, the novelty of this study lies in its detailed, holistic approach, providing a comprehensive understanding of sucrose and oil interactions by integrating molecular to macroscopic perspectives.

It is assumed that oil immobilization is affected, on the one hand, by the sucrose properties (such as particle size, morphology and specific surface area), and on the other hand, by the fatty acid (FA) composition

* Corresponding author at: Giggenhauser Str. 35, 85354 Freising, Germany.
E-mail address: hilke.schacht@ivv.fraunhofer.de (H. Schacht).

https://doi.org/10.1016/j.foodres.2025.115797
Received 17 July 2024; Received in revised form 14 January 2025; Accepted 18 January 2025
Available online 22 January 2025

of the edible oils. To investigate the interactions between sucrose and oil and the influence of their properties, dispersions of four sucrose and four oil samples were analyzed for oil binding capacity, oil diffusion, flow behavior, and wettability at various length scales.

2. State of the art

2.1. Mechanisms behind oil immobilization

The exact mechanisms behind oil immobilization on macroscopic and molecular levels are still not understood. Mechanisms of oil immobilization might be physical entrapment, adsorption and absorption, which are explained in more detail in this section.

2.1.1. Physical entrapment – Microscopic interactions

Physical entrapment of oils is caused by the crystallization of semi-solid or solid fats, such as palm oil or hydrogenated peanut oil. For example, in peanut butter or nougat pastes, these fats are added to form a network of fat crystals that entraps the liquid oil at least partially to avoid oil separation during storage (Aryana et al., 2003; Hubbes et al., 2020b). Another example are oleogels, where gelators such as waxes or mono-diglycerides are used to form a crystal network to entrap the oil. Although the oil inside this network remains liquid, oleogels have a semi-solid to solid texture (Blake et al., 2014; Trapp et al., 2023).

2.1.2. Oil sorption – Molecular interactions

Adsorption or absorption are two aspects of oil sorption leading to oil immobilization. Adsorption means that the triacylglycerides (TAGs) adhere on the surface of sorbents by mainly van der Waals forces without penetrating them. Lipophilic interactions or coalescence cause the accumulation of TAGs on the surface (Abdelwahab et al., 2017; Ifelebuegu and Johnson, 2017).

When oil penetrates into the pore spaces of a sorbent driven by capillary forces, this is referred to as absorption (Ifelebuegu and Johnson, 2017). For example, during deep-frying of potatoes, the frying oil penetrates the surface of the potatoes and is absorbed into their porous microstructure (Lumanlan et al., 2020). In addition, porous materials like starch exhibit high oil absorption capacities due to the presence of micro-sized pores, which increase its internal surface area (Purwitasari et al., 2023).

2.2. Characteristics of sucrose influencing oil immobilization

2.2.1. Particle size and surface area

The properties of sucrose particles in a dispersion play an important role regarding oil immobilization. Smaller sucrose particles have larger surface areas, resulting in a higher number of “oil adsorption sites” (Müller, 2010; Ziegler and Hogg, 2017). Mongia and Ziegler (2000) has shown that increasing the proportion of coarse particles relative to fine particles reduces both the yield value and plastic viscosity of chocolate. This was due to the lower surface area of coarse particles, which leaves more fat available as a flowing agent. Middendorf (2015) contradicted these results, showing that larger sucrose particles immobilized more cocoa butter than smaller ones, as larger void spaces between the sucrose particles were available for the entrapment of cocoa butter. However, recent findings confirmed that the viscosity of cocoa butter-sucrose-suspensions increases with the Brunauer-Emmett-Teller (BET) surface of sucrose, indicating a stronger interaction with the surrounding fat (Franke et al., 2024).

2.2.2. Density and porosity

Porosity is a measure of the void spaces in a material and is inversely related to its density. The lower the density and the higher the porosity of a solid is, the more oil can absorb due to more or larger hollow spaces (Ifelebuegu and Johnson, 2017). Pores are categorized according to their inner diameters into micropores (<2 nm), mesopores (2–50 nm) and macropores (>50 nm) (Sing, 1985). On the one hand, the pores must be large enough for TAGs to enter them, which are about 1.5–3 nm in diameter (Schultz and Solomon, 1961; Liljeblad et al., 2014). On the other hand, TAGs remain mobile in pores and can escape from them if the pores are too large, likely due to their smaller surface-to-volume ratio (Zhenxue et al., 2020; Zhang et al., 2022).

In addition, it is not only the porosity of the particles themselves that plays a role, but also the void volume in a bed of solid particles. The void volume is determined by the particle packing ability, which in turn, is influenced by the particle shape, size distribution, and packing arrangements. In chocolate, for example, molten fat fills the void spaces between the solid particles, resulting in an enhanced flowability (Mongia and Ziegler, 2000).

2.2.3. Crystalline and amorphous structure

In a crystalline structure, molecules of sucrose are arranged in a highly ordered and repetitive pattern, forming distinct crystal lattices. Crystalline sucrose is typically found in granular or powdered sugar. In contrast, an amorphous structure lacks the long-range molecular order. Amorphous sucrose is often found in candies, where rapid cooling prevents crystallisation (Krüger, 2017; Dadmohammadi and Datta, 2020; Ueda et al., 2023).

2.2.4. Polarity

The adsorption of oil molecules is related to a sorbent’s surface polarity (Freitas et al., 2007; Barthlott et al., 2020). As sucrose crystals have a polar surface (hydrophilic), they interact weakly with non-polar oil molecules, primarily by van der Waals forces (Abdelwahab et al., 2017; Ifelebuegu and Johnson, 2017). However, the adsorption of oil on the surface of polar sorbents can be enhanced by making the surface more hydrophobic, for example by large organic cations (Freitas et al., 2007). On the other hand, sucrose tends to agglomerate in oil-continuous dispersions to minimize the contact of their polar surface with the non-polar oil. This leads to void spaces, in which the oil molecules could potentially be entrapped (Windhab, 2000; Argudo et al., 2022).

2.3. Characteristics of oils influencing oil immobilization in dispersed systems

The FA composition of oils affects most of its properties, such as viscosity, melting point or surface tension. The viscosity and melting point of oils increase with the degree of saturation and the length of the FA chains (Bockisch, 2015). The higher the proportion of unsaturated FAs in oils, the greater their mobility (Truyen and Örsi, 1977). In addition, smaller TAGs with shorter FA chains have a higher mobility (Schultz and Solomon, 1961; Skytte and Kaylegian, 2017).

Furthermore, oil immobilization by adsorption is affected by the surface tension of oil. In general, the surface tension of plant oils is low compared to water. However, polar minor components and longer FA chains increase their surface tension (Melo-Espinosa et al., 2014; Sahasrabudhe et al., 2017; Scharfe et al., 2019). The polar sucrose surface likely enhances oil adhesion with higher surface tension (Wolf, 1957).

Interactions also take place between the TAGs themselves, primarily via van der Waals forces and hydrophobic interactions. Van der Waals forces contribute to the aggregation of TAGs, promoting cohesion within the liquid. Hydrophobic interactions arise in the presence of polar substances and can lead to droplet formation or coalescence in oil systems, affecting properties like viscosity and stability (Ben-Amotz, 2016).

3. Materials and methods

3.1. Materials

3.1.1. Sucrose

All sucrose samples were white refined sugars from sugarcane with a polarization of min. 99.7 °Z. Powdered sucrose (PS), granular fine sucrose (GFS) and granular coarse sucrose (GCS) (Pfeifer & Langen GmbH & Co. KG, Cologne, Germany) exhibited crystalline structures (Fig. S1, Supplementary). Cotton candy (CC) was produced in-house from GCS using a CC machine (Kesser®, Yeşil Yayla, Osmangazi, Turkey) and consisted of amorphous sucrose (Fig. S1, Supplementary). To preserve its amorphous structure, humidity was excluded using a glove box flooded with dry compressed air during production and air-tight containers in a desiccator with silica gel for storage.

The main properties of the sucrose samples in this work are summarized in Table 1. Methods and detailed results are shown in the Supplementary material. The particle size distribution of GCS and GFS was partially overlapping (Fig. S2, Supplementary).

GCS and GFS consisted of cubic crystals with sharp edges and uniform shapes (Fig. S3A–D, Supplementary). PS showed a slightly rounded shape with many agglomerates (Fig. S3E–F, Supplementary). CC consisted of long strands (typical lengths: 200 μm–3 mm, diameter: 13 μm, Fig. S4, Supplementary) with a smooth surface, some of which were interconnected (Fig. S3G–H, Supplementary). The CC strands were not hollow inside but filled. As all sucrose samples contained minimal moisture, its influence on oil immobilization is unlikely.

3.1.2. Oils

The main properties of refined coconut oil (CNO) from medium-chain triacylglycerides (MCT) (IOI Oleo GmbH, Wittenberge, Germany), refined peanut oil (PNO) (AAK, Hull, UK), refined sunflower oil (SFO) (Nestlé Deutschland AG, Neuss, Germany) and refined rapeseed oil (RSO) (VOG AG, Linz, Germany) in this work are summarized in Table 2.

During the refining process, minor components are largely removed (Table 2). Therefore, their effect on oil immobilization is improbable in this study. The effective mean diffusion coefficients ($\langle D_{eff} \rangle$) and the effective root-mean square displacement (z) of the oils were in the following order: PNO < RSO < SFO < MCT-CNO (Fig. S5, Supplementary) and correlated inversely with their viscosities (Table 2).

3.2. Methods

3.2.1. Preparation of sucrose-in-oil dispersions

To analyze the interactions between oil and sucrose, dispersions were prepared with 55 g of each oil (MCT-CNO, PNO, RSO or SFO) and 45 g of each sucrose (GCS, GFS, PS, or CC) using a Thermomix TM6 (Vorwerk, Wuppertal, Germany) for 15 min at room temperature (Fig. S6, Supplementary). These concentrations have been identified in preliminary tests as being optimal for the desired analyses in terms of texture.

The particle size distribution and morphologies of GCS, GFS and PS were not affected by the mixing process with oil, whereas the CC strands were partially shortened to lengths of approximately 25–500 μm (Fig. S7, Supplementary). The samples were stored air-tight under exclusion of light at room temperature.

Table 1
Physical and structural properties of sucrose samples.

Sucrose	Particle size distribution			Other physical and structural properties		
	d_{10} (μm)	d_{50} (μm)	d_{90} (μm)	ρ_b (g·cm^{-3})	BET surface (m^2·g^{-1})	Moisture (mg·g^{-1})
GCS	147.8 ± 2.1	239.3 ± 4.4	369.8 ± 9.0	0.88 ± 0.01	0.03 ± 0.01	0.40 ± 0.06
GFS	121.5 ± 1.6	193.5 ± 2.7	297.2 ± 4.6	0.81 ± 0.01	0.05 ± 0.01	0.03 ± 0.06
PS	11.9 ± 0.2	36.3 ± 0.5	101.8 ± 2.7	0.49 ± 0.02	0.53 ± 0.02	0.00 ± 0.00
CC	–	–	–	–	0.20 ± 0.07	0.70 ± 0.01

Values are expressed as mean with empirical SD of three replicates.

Table 2
Physicochemical properties of the oils.

FA (%)	MCT-CNO	PNO	RSO	SFO
8:0	58.2 ± 0.4	0.0 ± 0.0	0.0 ± 0.0	0.0 ± 0.0
10:0	38.3 ± 0.4	0.0 ± 0.0	0.0 ± 0.0	0.0 ± 0.0
12:0	3.5 ± 0.0	2.2 ± 0.2	1.4 ± 0.1	1.0 ± 0.0
16:0	0.0 ± 0.0	7.0 ± 0.1	4.9 ± 0.2	6.0 ± 0.0
18:0	0.0 ± 0.0	1.7 ± 0.0	1.6 ± 0.2	3.7 ± 0.0
18:1	0.0 ± 0.0	70.9 ± 0.3	61.7 ± 1.0	36.1 ± 0.2
18:2	0.0 ± 0.0	14.7 ± 0.0	19.8 ± 0.3	49.6 ± 0.1
18:3	0.0 ± 0.0	0.2 ± 0.2	7.8 ± 0.1	0.0 ± 0.0
22:0	0.0 ± 0.0	0.9 ± 0.0	1.1 ± 0.4	0.3 ± 0.4
other	0.0 ± 0.0	2.4 ± 0.0	1.4 ± 0.4	3.4 ± 0.3
Free FAs (mg·kg^{-1})	0.06 ± 0.01	0.03 ± 0.01	0.02 ± 0.01	0.03 ± 0.00
Monoglycerides (mg·g^{-1})	4.20 ± 0.20	2.80 ± 0.20	4.40 ± 0.20	5.90 ± 0.20
Diglycerides (mg·g^{-1})	8.50 ± 0.10	2.30 ± 0.10	8.60 ± 0.10	1.40 ± 0.10
Phosphorus (mg·g^{-1})	< 0.01*	< 0.01*	< 0.01*	< 0.01*
Moisture (mg·g^{-1})	0.03 ± 0.06	0.27 ± 0.06	0.00 ± 0.00	0.50 ± 0.00
Surface tension (mN·m^{-1})	29.21 ± 0.06	32.39 ± 0.06	32.75 ± 0.02	33.03 ± 0.02
Viscosity at 20 °C (mPa·s)	31.4 ± 0.6	84.9 ± 0.2	74.7 ± 0.6	68.7 ± 0.1

The relative amount of FA percentages refers to all measured FA from C4:0 to C24:0.
*Detection limit of the method.
Values are expressed as mean with empirical SD of three replicates.

3.2.2. Oil binding capacity (OBC) of sucrose-in-oil dispersions

The OBC indicates how much oil a substance can retain after the application of centrifugal force. The centrifugation tubes were weighed before (m_A) and after adding about 15 g dispersion (m_B). The filled tubes were centrifuged with a 3 K30 centrifuge (Sigma, Osterode, Germany) for 30 min at 5000 min^{-1} and 20 °C. The tubes were then placed upside down for 30 min, and the released oil was collected. The tubes were weighed again (m_C) to calculate OBC with Equation (1) and Equation (2).

$$c_{Releasedoil}(\%) = \frac{(m_B - m_A) - (m_C - m_A)}{(m_B - m_A)} \bullet 100 \quad (1)$$

$$OBC(\%) = 100 - c_{Releasedoil} \quad (2)$$

3.2.3. Diffusion of oil in sucrose-in-oil dispersions

The translational mobility of oil, i.e. molecular diffusion, in sucrose-in-oil dispersions was measured using ^{1}H PFG-STE NMR (pulsed field gradient-stimulated echo nuclear magnetic resonance) (Tanner, 1970) to investigate how oil diffusion is affected by the presence of sucrose depending on the particle size and inter-particle fractional volumes.

The diffusion experiments were performed at 20 °C on a 400 MHz spectrometer (Avance Neo WB ultrashield, Bruker BioSpin, Germany) equipped with a 5 mm DiffBB broadband gradient probe. The main experimental parameters of the PFG-STE sequence were: gradient pulse duration $\delta = 2.5$ ms; number of gradient steps: 32; number of averages 8; repetition time $t_R = 2$ s. Diffusion time Δ was varied in a series of 9 experiments between 0.02 and 0.4 s. ^{1}H NMR signals were quantified as a function of gradient amplitude in the range [0.38, …, 12.00] Tm^{-1}. To

determine the diffusion behavior, total integrals of the ^{1}H NMR spectra were processed via the bimodal distribution approach, which leads to two effective mean diffusion coefficients $\langle D_{\mathrm{eff,i}}\rangle$, the distribution widths σ_i and amplitudes A_i (Röding et al., 2012, 2015). The Einstein-Smoluchowski equation for the one-dimensional cases was used to calculate the effective root-mean square displacement z_i of the oil molecules, which depends on Δ and $\langle D_{\mathrm{eff,i}}\rangle$.

Geometric restriction of the oil diffusion path leads to a decrease of the diffusion coefficient, and an attempt was made to estimate the size of the liquid filled fractional volumes or voids by assuming a spherical geometry. This crude assumption allows for the application of the approach of Murday and Cotts (1968), Packer and Rees (1972) and Neuman (1974), which is usually used to determine the droplet size distribution in emulsions. The result is the effective volume-weighted mean diameter $d_{33,\mathrm{eff}}$ and the corresponding distribution width σ. $d_{33,\mathrm{eff}}(\Delta)$ is a measure of how well the model can be used for sizing the liquid filled fractional volumes in sucrose-in-oil dispersions and provides information about the geometric restriction of the oil by the sucrose particles. If $d_{33,\mathrm{eff}}$ is independent of Δ, the model describes the restriction in closed inter-particle pores, in the opposite case, the μm-scale voids are connected (open pores) or differ from the assumed spherical geometry significantly.

3.2.4. Viscosity of sucrose-in-oil dispersions

The flow curves of the dispersions were determined using a Rheometer Physika MCR 301 (Anton Paar, Ostfildern, Germany) with heating mantle (H-PTD200, Anton Paar, Ostfildern, Germany). A plate-plate geometry with a diameter of 25 mm (PP25/TG) and the TruGap™ function was used for the sucrose-in-oil dispersions. The samples were pre-tempered for 2 h at the measuring temperature of 20 °C. The flow curves were determined with an increasing shear rate from 0.1 to 100 s^{-1}.

3.2.5. Wettability

The wettability of the sucrose samples with the oils was analyzed using a self-build wetting scale (Fig. 1), which was modified following the method of Fitzpatrick et al. (2017). The construction consists of a scale, a closable aperture for the solids and a glass vessel (⌀ 75 mm) with 200 ml of oil. The closed aperture was filled with 1–2.5 g sucrose in loose bulk and smoothed out with a spatula. The aperture was opened, and the time required for the particles to be completely wetted by the oil was measured at room temperature. The oil was replaced after each test.

The normalized wetting time (t_{norm}) of the sucrose samples was calculated using Equation (3), where t_{real} is the measured wetting time, m is the standardized weight of 1 g and m_{real} is the real sample weight.

$$t_{norm} = t_{real} * \frac{m}{m_{real}} \tag{3}$$

3.2.6. Statistical analysis

All measurements, except for NMR analyses, were performed at least in triplicate. Mean values and empirical standard deviations (SD) were calculated well knowing that their statistical relevance is questionable, they are therefore used as indicators of errors. The HF-NMR device error was below 5 %.

4. Results

The detailed characterization of the sucrose samples (Section 3.1.1.) and the oils (Section 3.1.2.) provides the physicochemical properties of the components of the sucrose-in-oil dispersions as a basis (see also Supplementary). The immobilization of oils by sucrose particles and strands was analyzed at different length scales (molecular to macroscopic level) by OBC, molecular diffusion, flow behavior, viscosity and wettability.

4.1. Oil binding capacity (OBC)

At a macroscopic level, dispersions containing CC showed the highest OBC of up to 100 %, followed by PS (Fig. 2). GCS and GFS both had the lowest OBC and differed only in dispersions containing RSO. Dispersions with PS and GCS showed the lowest OBC with RSO compared to the other oils.

The exceptionally high OBC of CC may be attributed to a network-like structure of CC strands (Fig. S3G–H and Fig. S7, Supplementary), which could entrap the oil. The BET surface of CC was 4–7 times larger than GCS and GFS (Table 1), leading to an increased number of "oil adsorption sites" (Müller, 2010; Ziegler and Hogg, 2017; Basu and Sarkar, 2019). Another possible explanation could be the amorphous state of sucrose in CC (Fig. S1, Supplementary), which may result in increased void spaces for oil immobilization (Krüger, 2017; Ueda et al.,

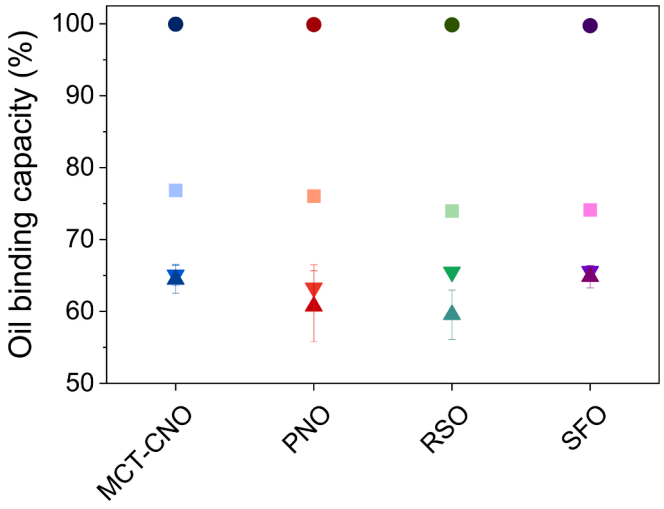

Fig. 2. Oil binding capacity (%) of sucrose-in-oil dispersions with MCT-CNO, PNO, RSO or SFO and sucrose samples marked by symbol: GCS (▲), GFS (▼), PS (■) and CC (●). Values are expressed as mean with empirical SD of three replicates.

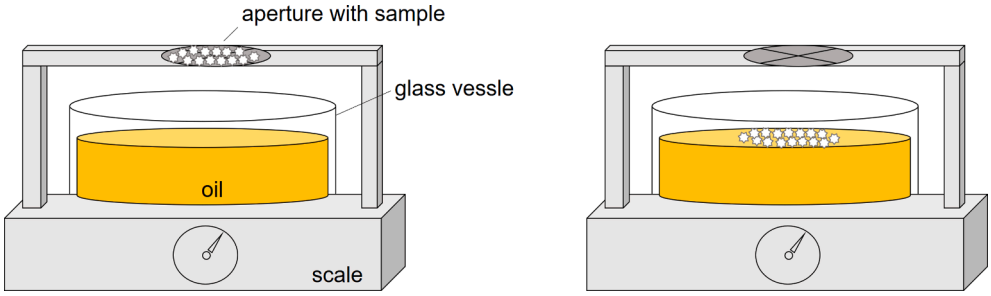

Fig. 1. Construction of the self-built wetting scale before and after opening the aperture.

2023). Oil absorption into the interior of the strands via capillary forces can, however, be excluded, as SEM images indicated that they are not hollow (Fig. S3G–H, Supplementary).

PS exhibited a significantly larger OBC than GCS and GFS, possibly due to its BET surface being more than 10 times larger (Table 1). In addition, the lower bulk density and mean particle size of PS compared to GCS and GFS (Table 1) indicated more and smaller cavities between the particles of PS, in which oil could possibly be trapped. This is consistent with the numerous agglomerates of PS particles observed in the SEM images (Fig. S3E–F, Supplementary), which contain void spaces (Windhab, 2000; Argudo et al., 2022).

In contrast, the cubic crystals of GCS and GFS were less capable of adhering tightly to one another, reducing the formation of such voids (Fig. S3A–D, Supplementary). In addition, GCS and GFS both consist of larger particles and have a lower BET surface compared to PS (Table 1), resulting in less "oil adsorption sites". The similar OBC of dispersions with GCS and GFS could be explained by the partially overlapping particle size distribution (Fig. S2, Supplementary) and the similar morphology (Fig. S3A–D, Supplementary) and BET surface (Table 1).

As no large differences between the oils were observed, we conclude that the OBC was stronger influenced by the sucrose properties than by oil properties.

4.2. Diffusion of oil in dispersions

SFO was used as an example to demonstrate oil diffusion in sucrose-in-oil dispersions on a molecular length scale (Fig. 3). Two mean effective diffusion coefficients $\langle D_{eff,1}\rangle$ (Fig. 3A) and $\langle D_{eff,2}\rangle$ (Fig. 3B) and their distribution widths σ_1 and σ_2 are required to describe the signal decays in PFG experiments of SFO in the sucrose-in-oil dispersions sufficiently well: A fraction A_1 (Fig. 3C) of SFO that diffuses faster ($\langle D_{eff,1}\rangle \in [0.6, \ldots, 1.1]\bullet 10^{-11}$ m^{2}s^{-1}) and a fraction A_2 (Fig. 3D) that diffuses more slowly ($\langle D_{eff,2}\rangle \in [0.9, \ldots, 9.0]\bullet 10^{-12}$ m^{2}s^{-1}). In contrast to the sucrose-in-oil dispersions with GCS, GFS and CC ($A_1 \approx 0.65$), A_1 in dispersions with PS ($A_1 \approx 0.47$) is in the same order of magnitude than A_2 ($A_2 \approx 0.53$).

$\langle D_{eff,1}\rangle$ and $\langle D_{eff,2}\rangle$ decrease with increasing Δ, which indicates hindered diffusion in the dispersions. The decrease in $\langle D_{eff,2}\rangle$ with

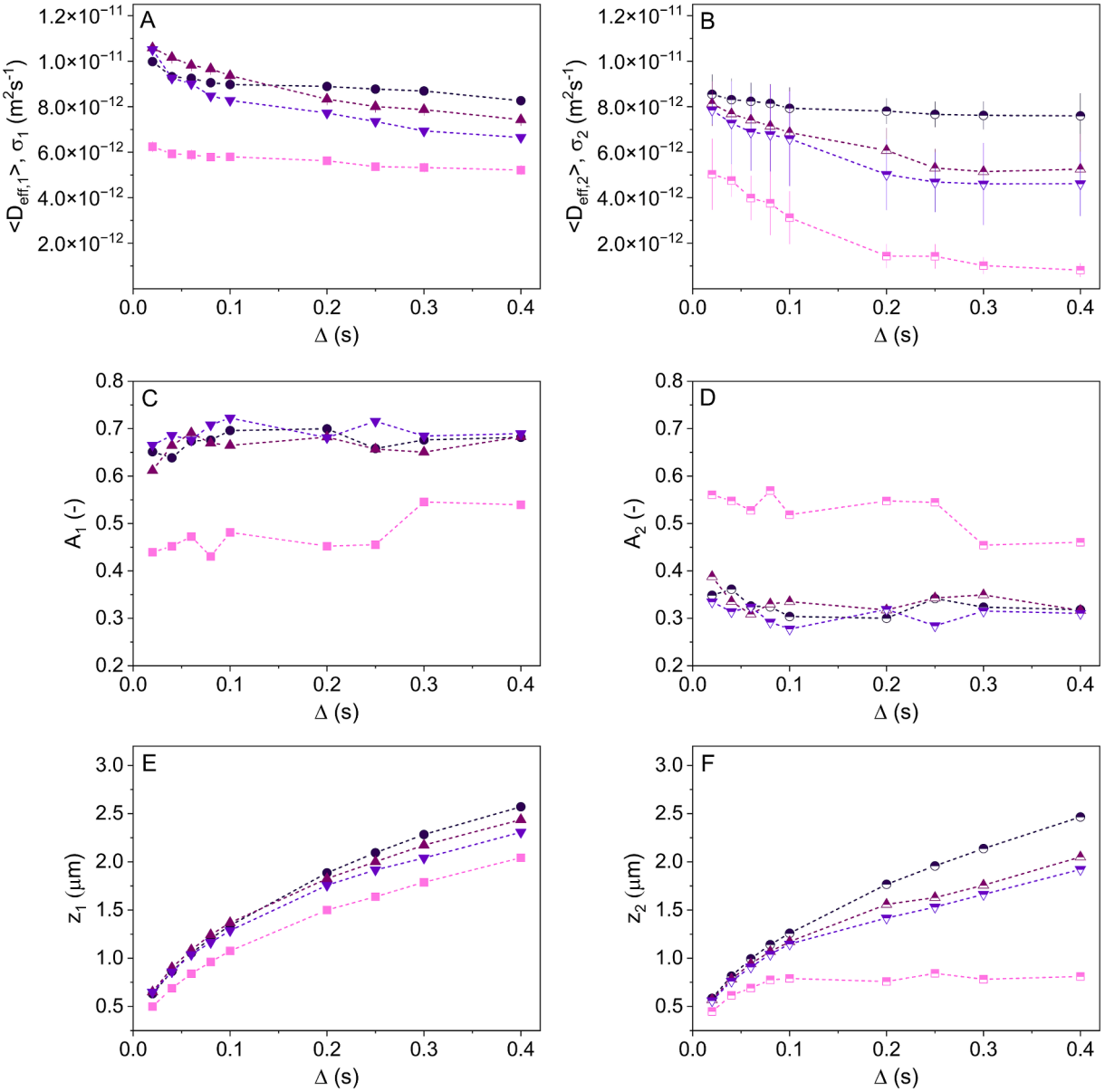

Fig. 3. SFO in sucrose dispersions: **(A)** $\langle D_{eff,1}\rangle$ and **(B)** $\langle D_{eff,2}\rangle$ with σ_1 and σ_2 (vertical lines), respectively, **(C)** A_1 and **(D)** A_2, and **(E)** z_1 and **(F)** z_2 as a function of Δ, GCS (▲), GFS (▼), PS (■), and CC (●). In **(A)**, σ is smaller than the size of the data point symbols ($\sigma \approx 10^{-16}$ m^2 s^{-1}).

increasing Δ is larger than that of $\langle D_{eff,1} \rangle$, again especially for PS. In sucrose-in-oil dispersions with CC, the decrease with increasing Δ is the smallest, which indicates a smaller geometric hindrance in CC + SFO compared to the others at the molecular scale. The mean diffusion length z is largest for sucrose-in-oil dispersions with CC, while z is smallest for the sugar-in-oil dispersions with PS (Fig. 3E, F).

In analogy to the findings in oleogels (Trapp et al., 2023), the two fractions could be attributed to oil molecules near the sucrose surfaces indicating interactions / adsorption (A_2, $\langle D_{eff,2} \rangle$), while the A_1 fraction describes oil molecules in quasi free environments in the voids at large distances from the particles' surfaces with less pronounced Δ dependence. This interpretation is supported by the fact that the surface-to-volume ratio is the largest for PS among the investigated dispersions.

In addition to diffusion coefficients, the measurements also provide information about the length scales of a dispersed system. According to Murday and Cotts (1968), Packer and Rees (1972) and Neuman (1974), the characteristic size between the sugar particles was estimated assuming a spherical geometry (Fig. 4). For the sucrose-in-oil dispersions with GCS, GFS and PS, a similar dependence of $d_{33,eff}$ on Δ is observed. The increase in $d_{33,eff}$ with increasing Δ is however significantly larger for the sucrose-in-oil dispersions with CC. This shows that the CC strands form an open pore structure and therefore the data are hardly describable via the assumption of a spherical pore shape. The oil in this system diffuses less geometrically restricted. The other extreme is the PS dispersion with the smallest effective length scale of the liquid filled fractional volumes in the order of 2–3 μm. The information derived from Fig. 4 about the geometry of the liquid filled fractional volumes is consistent with the observations in the SEM images (Fig. S3, Supplementary), the particle size distributions (Table 1 and Fig. S2, Supplementary), but also with the viscosity measurements (Table 1). In summary, the results confirm that oil immobilization on a molecular level is affected by the morphology of sucrose.

4.3. Flow behavior and viscosity

The rheometric measurements of sucrose-in-oil dispersions provide insight into the flow characteristics and internal structure of the oil within the dispersions at microscopic to macroscopic levels. Dispersions containing CC showed the highest viscosities, especially at low shear, followed by dispersions with PS (Fig. 5). Both behaved in a shear-thinning manner with all tested oils in contrast to GFS and GCS dispersions. Dispersions containing PNO or RSO (Fig. 5 B, C) exhibited higher viscosities with GCS compared to GFS, whereas no differences were observed between these two sucrose samples with MCT-CNO or SFO (Fig. 5 A, D).

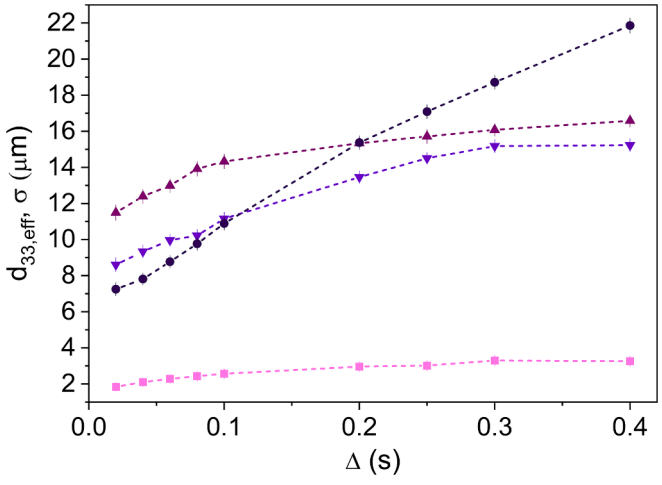

Fig. 4. $d_{33,eff}$ and σ using the approach of Murday and Cotts (1968), assuming a spherical geometry as a function of Δ exemplarily for the sucrose-in-oil dispersion with SFO and GCS (▲), GFS (▼), PS (■) or CC (●), which allowed for an estimate of the order of magnitudes of the liquid filled fractional volumes. σ is partly in the order of the data point symbols (σ ≈ 0.7 μm).

MCT-CNO led to higher viscosities of the dispersions with CC and PS compared to the other oils (Fig. 5).

Although pure MCT-CNO without sucrose exhibited the significantly lowest viscosity among all oils (Table 2), it resulted in the highest viscosities in dispersions with CC and PS, especially at low shear (Fig. 5). This is due to the smaller TAGs of MCT-CNO, which consist solely of saturated medium-chain FAs (Table 2) with a linear molecular conformation. These TAGs likely adhere to or adsorb more effectively onto the sucrose surface compared to TAGs with unsaturated long-chain FAs. PNO without sucrose exhibited the highest viscosity among all oils (Table 2) and resulted in the second highest viscosities in sucrose dispersions at low shear. This could be due to the higher content of saturated FAs (Table 2).

The viscosities of the sucrose-in-oil dispersions are in accordance with their OBC (Fig. 2). Dispersions with high OBC, particularly those with CC, also exhibit the highest viscosities. This correlation highlights that the immobilized oil fraction is not available for the flow process, thereby reducing flowability and leading to an increased viscosity (Windhab, 2000; Middendorf, 2015; Ziegler and Hogg, 2017; Franke et al., 2024). In particular, the shear-thinning behavior of dispersions with CC and PS indicates the formation of sucrose-oil networks, which were disrupted under shear forces.

4.4. Wettability

Wettability provides information into how well the oil interacts with or adheres to the sucrose surface on a macroscopic level. PS and CC needed the longest time to be wetted with oil, while GCS and GFS were wetted equally fast (Table 3). MCT-CNO showed a much shorter wetting time with PS and CC compared to PNO, RSO and SFO.

The long wetting time of PS is due to the agglomeration of PS particles in the oil phase to minimize the contact of their polar surface with the non-polar oil (Windhab, 2000; Argudo et al., 2022). The formation of agglomerates of PS is reflected by its 10 times higher BET surface compared to GCS and GFS. CC has a similar BET surface to PS and a comparable wetting time. In contrast, GCS and GFS interacted less with the surrounding oil due to their larger particles, which is also reflected in their smaller BET surface (Table 1).

The faster wetting of PS and CC with MCT-CNO, compared to the other oils, is consistent with the viscosity measurements. This supports the assumption that the medium-chain TAGs of MCT-CNO adhere more effectively to the surface of PS and CC.

4.5. Correlation of measurement results on different length scales

The correlated view of data from different methods measuring oil mobility on various length scales and from different perspectives, as shown by dispersions with SFO (Fig. 6), provides comprehensive insight and establishes connections between the measurements.

Dispersions with a high OBC, particularly those containing CC, also exhibit larger viscosities. This suggests that the immobilized oil reduces the amount of mobile or "free" oil available for flow, thereby increasing viscosity and promoting the formation of sucrose-oil networks – apart from the known effect of size and shape of the sucrose particles on rheologic properties.

While CC exhibited the highest oil immobilization on the macroscopic scale (OBC and rheology), oil diffusion was least hindered by CC on the molecular scale (μm). This highlights the importance of considering the respective measurement methods' length scales when interpreting the results. The combination of these findings suggests that most of the oil was physically entrapped within the CC network, rather than adsorbed onto the surface of the CC strands, as it diffused most freely within the network while this dispersion also exhibited the highest oil

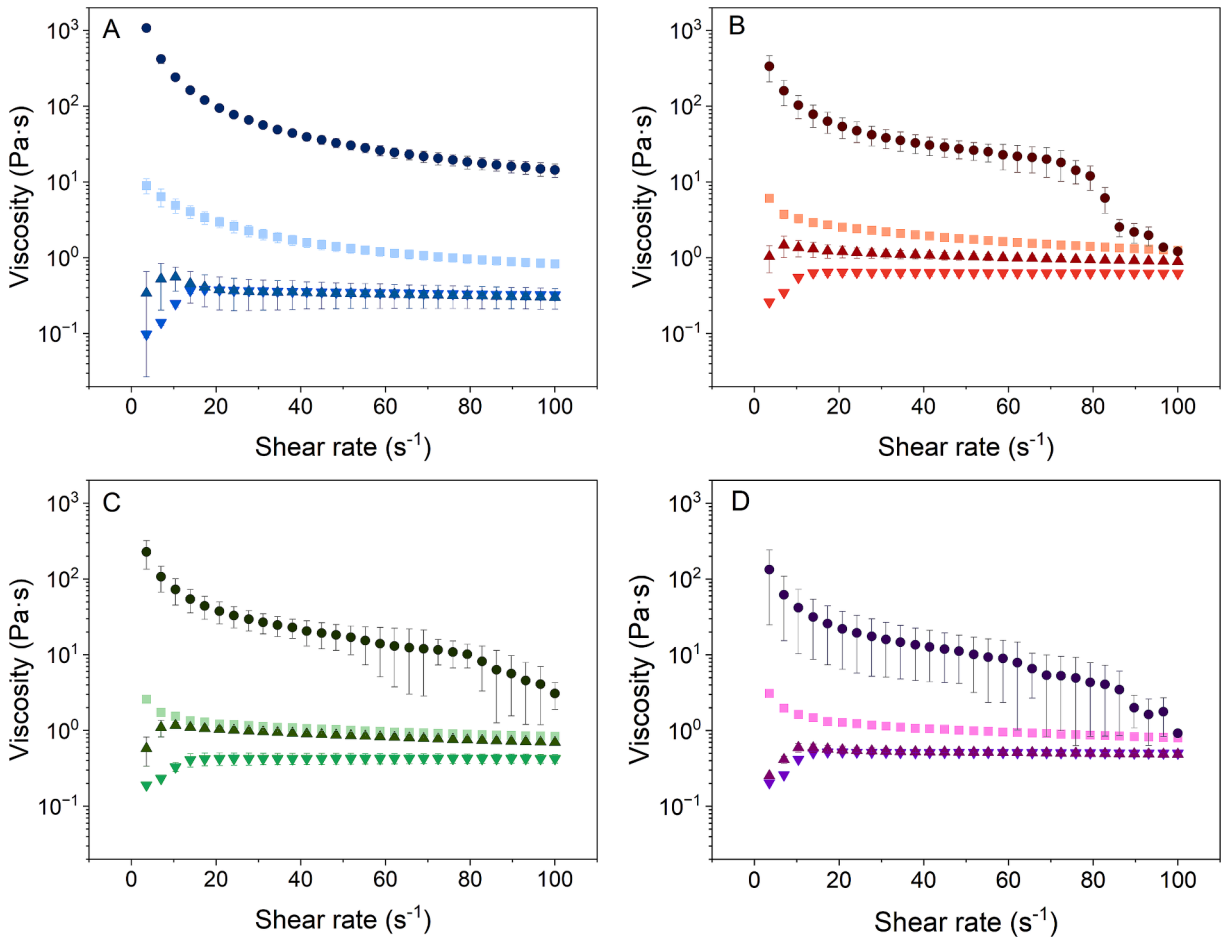

Fig. 5. Flow curves of sucrose-in-oil dispersions with (**A**) MCT-CNO, (**B**) PNO, (**C**) RSO or (**D**) SFO and sucroses marked by symbols: GCS (▲), GFS (▼), PS (■) or CC (●). Values are expressed as mean with empirical SD of three replicates.

Table 3
Wettability of sucrose samples with refined oils.

	Normalized wetting time (s)			
Sample	MCT-CNO	PNO	RSO	SFO
GCS	1.6 ± 0.3	1.5 ± 0.3	1.2 ± 0.3	2.3 ± 0.6
GFS	1.2 ± 0.3	4.0 ± 0.5	3.8 ± 0.5	3.3 ± 0.3
PS	44.7 ± 4.3	101.9 ± 3.5	101.7 ± 6.9	96.0 ± 2.3
CC	32.9 ± 9.9	108.9 ± 10.1	119.3 ± 5.1	110.8 ± 9.4

Values are expressed as mean with empirical SD of three replicates.

immobilization on a macroscopic scale. As the CC network showed an open structure (Fig. 4), the oil still diffused freely over certain distances within these network's interstitial spaces. We conclude that the viscosity measured on the macroscopic length scale is mainly determined by the size and shape of CC.

The prolonged wetting times, higher OBC and viscosities for CC and PS correlate with their reticulated structures or agglomerated particles and larger BET surface, which enhance oil interactions and immobilization. In case of PS, these properties also contribute to lower $\langle D_{\mathrm{eff}} \rangle$ within the dispersion, reflecting more pronounced geometric restrictions imposed by the small PS particles, which leads to small void sizes. Wetting times are also expected to be larger for structures with smaller pore sizes.

GFS and GCS exhibit shorter wetting times, lower OBC, and reduced viscosities. These results suggest weaker oil interactions, which can be attributed to larger particle, and in consequence larger pore sizes, smaller BET surface areas, and less structured networks, owing the cubic crystal particle shape. Therefore, oil diffusion is less hindered in these dispersions, resulting in larger $\langle D_{\mathrm{eff}} \rangle$ compared to dispersions with PS.

By linking these datasets, the analysis highlights the crucial role of sucrose particle shape, size, and BET surface in controlling oil immobilization.

5. Conclusion

In this study, the impact of sucrose and oil characteristics on oil immobilization in dispersions was investigated in a holistic approach, providing a comprehensive understanding of their interactions by considering molecular to macroscopic perspectives.

Oil immobilization was analyzed in sucrose-in-oil dispersions on a macroscopic level by centrifugation, rheometry and wettability, and on a molecular level by NMR diffusometry.

On a macroscopic level, cotton candy showed the highest oil immobilization, followed by powdered sucrose. The strands of cotton candy likely formed a reticulated structure, and the agglomerated particles of powdered sucrose led to more void spaces to entrap the oil, compared to the angular-shape crystals of both granular sucroses. This was also reflected in their larger BET surface compared to the granular sucrose samples, leading to more "oil adsorption sites".

On a molecular level, oil diffusion was hindered most by powdered sucrose, while the geometric hindrance was the lowest in dispersions with cotton candy. The oil diffused further distances within the open structure of the cotton candy network, while the void spaces between particles of powdered sucrose were narrower and thus allowed shorter distances of diffusion.

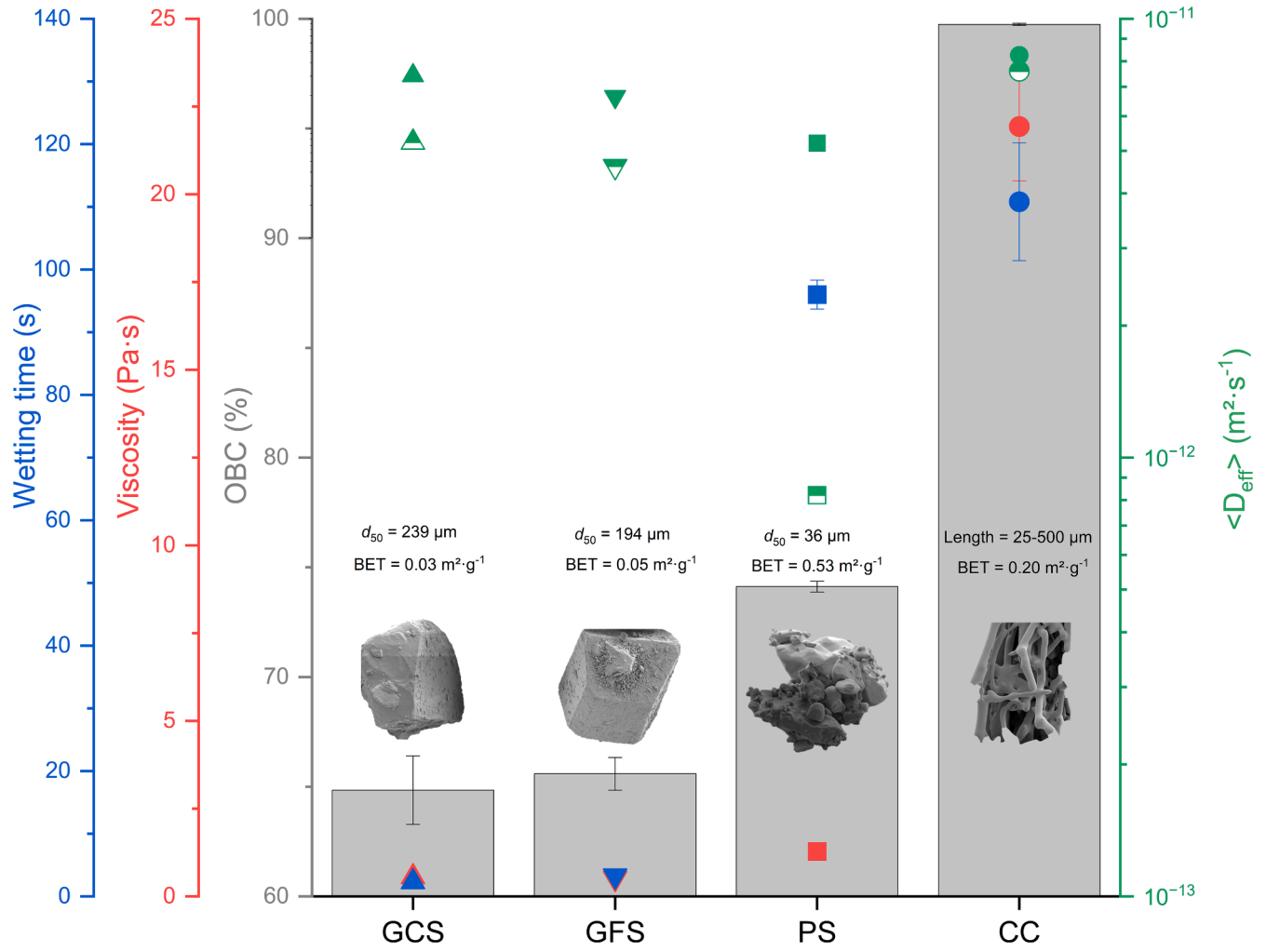

Fig. 6. Summary of the results obtained from the different methods for oil mobility, exemplarily shown for sucrose-in-oil dispersions with SFO. The methods are marked by color: wetting time (blue), viscosity at a shear rate of 20 s^{-1} (red), OBC (gray), and $\langle D_{eff,1} \rangle$ (filled symbols) and $\langle D_{eff,2} \rangle$ (half-filled symbols) (green) at Δ = 0.4 s. The sucrose samples are marked by symbols: GCS (▲), GFS (▼), PS (■), and CC (●).

The results highlight the importance of considering length scales of the respective measurement methods used for oil mobility as well as the properties of the constituents of dispersions. Future research will involve a comprehensive multi-block analysis to further elucidate the relationships and interactions within the sucrose-in-oil dispersions.

CRediT authorship contribution statement

Hilke Schacht: Writing – original draft, Visualization, Validation, Methodology, Investigation, Conceptualization. **Lena Trapp:** Writing – original draft, Visualization, Methodology, Investigation. **Maike Föste:** Writing – review & editing, Data curation, Conceptualization. **Isabell Rothkopf:** Writing – review & editing, Project administration, Conceptualization. **Gisela Guthausen:** Writing – review & editing, Writing – original draft, Supervision, Data curation, Conceptualization.

Funding

We thank the German Federation of Industrial Research Associations (AiF) for its financial support of the research project Nr. 21785N. This project was financed within the budget of the Federal Ministry for Economic Affairs and Climate Action (BMWK) for promoting the Industrial Collective Research (IGF). We also thank the Industrial Association for Food Technology and Packaging (IVLV) for its support of the project "Oil mobility".

Declaration of competing interest

The authors declare that they have no known competing financial interests or personal relationships that could have appeared to influence the work reported in this paper.

Acknowledgments

We thank the Chocolate Technology Working Group of the Industrial Association for Food Technology and Packaging (IVLV), Freising, Germany, for the joint discussion of experiments and results. We thank Valentin Haury, Michael Schott and Birgit Hillebrand for analytical assistance.

Appendix A. Supplementary material

Supplementary data to this article can be found online at https://doi.org/10.1016/j.foodres.2025.115797.

Data availability

Data will be made available on request.

References

Abdelwahab, O., Nasr, S. M., & Thabet, W. M. (2017). Palm fibers and modified palm fibers adsorbents for different oils. *Alexandria Engineering Journal, 56*, 749–755. https://doi.org/10.1016/j.aej.2016.11.020

Argudo, A., Zhou, L., & Rousseau, D. (2022). Sugar-sugar interactions in oil suspensions containing surfactants and effects on macroscopic phenomena. *Food Research International, 157*, Article 111217. https://doi.org/10.1016/j.foodres.2022.111217

Aryana, K., Resurreccion, A., Chinnan, M., & Beuchat, L. (2003). Functionality of palm oil as a stabilizer in peanut butter. *Journal of Food Science, 68*, 1301–1307. https://doi.org/10.1111/j.1365-2621.2003.tb09643.x

Babin, H., Dickinson, E., Chisholm, H., & Beckett, S. (2005). Interactions in dispersions of sugar particles in food oils: Influence of emulsifier. *Food Hydrocolloids, 19*, 513–520. https://doi.org/10.1016/j.foodhyd.2004.10.016

Barthlott, W., Moosmann, M., Noll, I., Akdere, M., Wagner, J., Roling, N., Koepchen-Thomä, L., Azad, M., Klopp, K., & Gries, T. (2020). Adsorption and superficial transport of oil on biological and bionic superhydrophobic surfaces: A novel technique for oil–water separation. *Philosophical Transactions of the Royal Society, 378*, Article 20190447. https://doi.org/10.1098/rsta.2019.0447

Basu, S., & Sarkar, J. (2019). Selective adsorption of oil on self-organized surface patterns formed over soft thin PDMS films. *Chemical Engineering Science, 207*, 970–979. https://doi.org/10.1016/j.ces.2019.07.021

Ben-Amotz, D. (2016). Water-mediated hydrophobic interactions. *Annual Review of Physical Chemistry, 67*, 617–638. https://doi.org/10.1146/annurev-physchem-040215-112412

Blake, A. I., Co, E. D., & Marangoni, A. G. (2014). Structure and physical properties of plant wax crystal networks and their relationship to oil binding capacity. *Journal of the American Oil Chemists' Society, 91*, 885–903. https://doi.org/10.1007/s11746-014-2435-0

Bockisch, M. (2015). Composition, structure, physical data, and chemical reactions of fats and oils and their associates. In M. Bockisch (Ed.), *Fats and oils handbook* (pp. 53–78). Elsevier.

Büschelberger, H.-G., Tirok, S., Stoffels, I., & Schöppe, A. (2015). Lecithins. In V. Norn (Ed.), *Emulsifiers in food technology* (p. 44). John Wiley & Sons.

Dadmohammadi, Y., & Datta, A. K. (2020). Food as porous media: A review of the dynamics of porous properties during processing. *Food Reviews International, 38*, 953–985. https://doi.org/10.1080/87559129.2020.1761376

Das, M., & Das, A. (2024). A comprehensive review on strategies for replacing saturated fats in bakery products. *Discover Food, 4*, Article 156. https://doi.org/10.1007/s44187-024-00240-2

Ereifej, K., Rababah, T., & Al-Rababah, M. (2005). Quality attributes of halva by utilization of proteins, non-hydrogenated palm oil, emulsifiers, gum arabic, sucrose, and calcium chloride. *International Journal of Food Properties, 8*, 415–422. https://doi.org/10.1080/10942910500267323

Fitzpatrick, J. J., Salmon, J., Ji, J., & Miao, S. (2017). Characterisation of the wetting behaviour of poor wetting food powders and the influence of temperature and film formation. *KONA Powder and Particle Journal, 34*, 282–289. https://doi.org/10.14356/kona.2017019

Franke, K., Bindrich, U., Schroeder, S., Heinz, V., & Middendorf, D. (2024). Changes of surface properties of sucrose particles during grinding in a cocoa butter-based suspension and their influence on the macroscopic behavior of the suspension. *European Food Research and Technology, 250*, 2353–2362. https://doi.org/10.1007/s00217-024-04542-8

Freitas, A., Mendes, M., & Coelho, G. (2007). Thermodynamic study of fatty acids adsorption on different adsorbents. *The Journal of Chemical Thermodynamics, 39*, 1027–1037. https://doi.org/10.1016/j.jct.2006.12.016

Hubbes, S.-S., Braun, A., & Foerst, P. (2020a). Sugar particles and their role in crystallization kinetics and structural properties in fats used for nougat creme production. *Journal of Food Engineering, 287*, Article 110130. https://doi.org/10.1016/j.jfoodeng.2020.110130

Hubbes, S.-S., Braun, A., & Foerst, P. (2020b). Crystallization kinetics and mechanical properties of nougat creme model fats. *Food Biophysics, 15*, 1–15. https://doi.org/10.1007/s11483-019-09596-w

Ifelebuegu, A. O., & Johnson, A. (2017). Nonconventional low-cost cellulose-and keratin-based biopolymeric sorbents for oil/water separation and spill cleanup: A review. *Critical Reviews in Environmental Science and Technology, 47*, 964–1001. https://doi.org/10.1080/10643389.2017.1318620

Johansson, D., & Bergenståhl, B. (1992a). The influence of food emulsifiers on fat and sugar dispersions in oils. I. Adsorption, sedimentation. *Journal of the American Oil Chemists Society, 69*, 705–717. https://doi.org/10.1007/BF02635905

Johansson, D., & Bergenståhl, B. (1992b). The influence of food emulsifiers on fat and sugar dispersions in oils. II. Rheology, colloidal forces. *Journal of the American Oil Chemists' Society, 69*, 718–727. https://doi.org/10.1007/BF02635906

Krüger, C. (2017). Sugar and bulk sweeteners. In S. T. Beckett, M. S. Fowler, & G. R. Ziegler (Eds.), *Beckett's industrial chocolate manufacture and use* (pp. 80–81). John Wiley & Sons Inc.

Liljeblad, J. F., Tyrode, E., Thormann, E., Dublanchet, A.-C., Luengo, G., Johnson, C. M., & Rutland, M. W. (2014). Self-assembly of long chain fatty acids: Effect of a methyl branch. *Physical Chemistry Chemical Physics, 16*, 17869–17882. https://doi.org/10.1039/C4CP00512K

Lumanlan, J. C., Fernando, W. M. A. D. B., & Jayasena, V. (2020). Mechanisms of oil uptake during deep frying and applications of predrying and hydrocolloids in reducing fat content of chips. *International Journal of Food Science & Technology, 55*, 1661–1670. https://doi.org/10.1111/ijfs.14435

Martínez, E., Pardo, J. E., Rabadán, A., & Álvarez-Ortí, M. (2023). Effects of animal fat replacement by emulsified melon and pumpkin seed oils in deer burgers. *Foods, 12*, Article 1279. https://doi.org/10.3390/foods12061279

Melo-Espinosa, E. A., Sánchez-Borroto, Y., Errasti, M., Piloto-Rodríguez, R., Sierens, R., Roger-Riba, J., & Christopher-Hansen, A. (2014). Surface tension prediction of vegetable oils using artificial neural networks and multiple linear regression. *Energy Procedia, 57*, 886–895. https://doi.org/10.1016/j.egypro.2014.10.298

Middendorf, D. (2015). Rasterkraftmikroskopische Untersuchungen zur Adsorption von Emulgatoren an Saccharosepartikeloberflächen in kakaobutterbasierten Suspensionen. *Technischen Universität Braunschweig.* https://doi.org/10.13140/RG.2.1.3642.2884

Mongia, G., & Ziegler, G. R. (2000). The role of particle size distribution of suspended solids in defining the flow properties of milk chocolate. *International Journal of Food Properties, 3*, 137–147. https://doi.org/10.1080/10942910009524621

Müller, B. R. (2010). Effect of particle size and surface area on the adsorption of albumin-bonded bilirubin on activated carbon. *Carbon, 48*, 3607–3615. https://doi.org/10.1016/j.carbon.2010.06.011

Murday, J., & Cotts, R. M. (1968). Self-diffusion coefficient of liquid lithium. *The Journal of Chemical Physics, 48*, 4938–4945. https://doi.org/10.1063/1.1668160

Neuman, C. (1974). Spin echo of spins diffusing in a bounded medium. *The Journal of Chemical Physics, 60*, 4508–4511. https://doi.org/10.1063/1.1680931

Packer, K., & Rees, C. (1972). Pulsed NMR studies of restricted diffusion. I. Droplet size distributions in emulsions. *Journal of Colloid and Interface Science, 40*, 206–218. https://doi.org/10.1016/0021-9797(72)90010-0

Purwitasari, L., Wulanjati, M. P., Pranoto, Y., & Witasari, L. D. (2023). Characterization of porous starch from edible canna (Canna edulis Kerr.) produced by enzymatic hydrolysis using thermostable α-amylase. *Food Chemistry Advances, 2*, Article 100152. https://doi.org/10.1016/j.focha.2022.100152

Röding, M., Bernin, D., Jonasson, J., Särkkä, A., Topgaard, D., Rudemo, M., & Nydén, M. (2012). The gamma distribution model for pulsed-field gradient NMR studies of molecular-weight distributions of polymers. *Journal of Magnetic Resonance, 222*, 105–111. https://doi.org/10.1016/j.jmr.2012.07.005

Röding, M., Williamson, N. H., & Nydén, M. (2015). Gamma convolution models for self-diffusion coefficient distributions in PGSE NMR. *Journal of Magnetic Resonance, 261*, 6–10. https://doi.org/10.1016/j.jmr.2015.10.001

Rothkopf, I., & Danzl, W. (2015). Changes in chocolate crystallization are influenced by type and amount of introduced filling lipids. *European Journal of Lipid Science and Technology, 117*, 1714–1721. https://doi.org/10.1002/ejlt.201400552

Sahasrabudhe, S. N., Rodriguez-Martinez, V., O'Meara, M., & Farkas, B. E. (2017). Density, viscosity, and surface tension of five vegetable oils at elevated temperatures: Measurement and modeling. *International Journal of Food Properties, 20*, 1965–1981. https://doi.org/10.1080/10942912.2017.1360905

Scharfe, M., Ahmane, Y., Seilert, J., Keim, J., & Flöter, E. (2019). On the effect of minor oil components on β-sitosterol/γ-oryzanol oleogels. *European Journal of Lipid Science and Technology, 121*, Article 1800487. https://doi.org/10.1002/ejlt.201800487

Schultz, S. G., & Solomon, A. (1961). Determination of the effective hydrodynamic radii of small molecules by viscometry. *The Journal of General Physiology, 44*, 1189–1199. https://doi.org/10.1085/jgp.44.6.1189

Shakerardekani, A., Karim, R., Ghazali, H. M., & Chin, N. L. (2013). The effect of monoglyceride addition on the rheological properties of pistachio spread. *Journal of the American Oil Chemists' Society, 90*, 1517–1521. https://doi.org/10.1007/s11746-013-2299-8

Sing, K. S. (1985). Reporting physisorption data for gas/solid systems with special reference to the determination of surface area and porosity (Recommendations). *Pure and Applied Chemistry, 57*, 603–619. https://doi.org/10.1351/pac198557040603

Skytte, U. P., & Kaylegian, K. E. (2017). Ingredients from milk. In S. T. Beckett, M. S. Fowler, & G. R. Ziegler (Eds.), *Beckett's industrial chocolate manufacture and use* (pp. 112–113). John Wiley & Sons Inc.

Tanner, J. E. (1970). Use of the stimulated echo in NMR diffusion studies. *The Journal of Chemical Physics, 52*, 2523–2526. https://doi.org/10.1063/1.1673336

Trapp, L., Schacht, H., Eymann, L., Nirschl, H., & Guthausen, G. (2023). Oil mobility in hazelnut oil-based oleogels investigated by NMR. *Applied Magnetic Resonance, 54*, 1445–1462. https://doi.org/10.1007/s00723-023-01571-6

Truyen, T. T., & Örsi, F. (1977). Die Fettsäure-Zusammensetzung des freien und gebundenen Fettes von Milchpulvern. *Molecular Nutrition & Food Research, 21*, 37–43. https://doi.org/10.1002/food.19770210106

Ueda, J. M., Morales, P., Fernández-Ruiz, V., Ferreira, A., Barros, L., Carocho, M., & Heleno, S. A. (2023). Powdered foods: Structure, processing, and challenges: A review. *Applied Sciences, 13*, Article 12496. https://doi.org/10.3390/app132212496

Vignolles, M.-L., Jeantet, R., Lopez, C., & Schuck, P. (2007). Free fat, surface fat and dairy powders: Interactions between process and product. A review. *Le Lait, 87*, 187–236. https://doi.org/10.1051/lait:2007010

Windhab, E. (2000). Fluid immobilization—A structure-related key mechanism for the viscous flow behaviour of concentrated suspension system. *Applied Rheology, 10*, 134–144. https://doi.org/10.1515/arh-2000-0009

Zhang, K., Jiang, Z., Song, Y., Jia, C., Yuan, X., Wang, X., Zhang, L., Han, F., Yang, Y., & Zeng, Y. (2022). Quantitative characterization for pore connectivity, pore wettability, and shale oil mobility of terrestrial shale with different Lithofacies - A case study of the Jurassic Lianggaoshan Formation in the Southeast Sichuan Basin of

the Upper Yangtze Region in Southern China. *Frontiers in Earth Science, 10*, Article 864189. https://doi.org/10.3389/feart.2022.864189

Zhenxue, J., Tingwei, L., Houjian, G., Tao, J., Jiaqi, C., Chuanxiang, N., Siyuan, S., & Weitao, C. (2020). Characteristics of low-mature shale reservoirs in Zhanhua Sag and their influence on the mobility of shale oil. *Acta Petrolei Sinica, 41*, Article 1587. https://doi.org/10.7623/syxb202012011

Ziegler, G. R., & Hogg, R. (2017). Particle size reduction. In S. T. Beckett, M. S. Fowler, & G. R. Ziegler (Eds.), *Beckett's industrial chocolate manufacture and use* (pp. 233–237). John Wiley & Sons Inc.